Research Article Vol. 31, No. 6 / 13 Mar 2023 / Optics Express 9760
Optics EXPRESS

Parametric amplification based on intermodal four-wave mixing between different supermodes in coupled-core fibers

MINJI SHI,[1] VITOR RIBEIRO,[1,2] AND AURO M. PEREGO[1,*]

[1]Aston Institute of Photonic Technologies, Aston University, Birmingham, B4 7ET, United Kingdom
[2]Kets Quantum Security Ltd., BS15 4PJ Bristol, UK
[*]a.perego1@aston.ac.uk

Abstract: Parametric amplifiers relying on the nonlinear four-wave mixing process are known for their signature symmetric gain spectrum, where signal and idler sidebands are generated on both sides of a powerful pump wave frequency. In this article we show analytically and numerically that parametric amplification in two identically coupled nonlinear waveguides can be designed in such a way that signals and idlers are naturally separated into two different supermodes, hence providing idler-free amplification for the supermode carrying signals. This phenomenon is based on the coupled-core fibers analogue of intermodal four wave-mixing occurring in a multimode fiber. The control parameter is the pump power asymmetry between the two waveguides, which leverages the frequency dependency of the coupling strength. Our findings pave the way for a novel class of parametric amplifiers and wavelength converters, based on coupled waveguides and dual-core fibers.

Optical parametric amplifiers are promising devices for signal amplification and wavelength conversion [1,2]. The physical principle underpinning their operation is four-wave mixing mediated by Kerr nonlinearity in presence of a powerful pump wave [3]. They have been demonstrated in silica fibers [2] and in integrated waveguides too [4–6]. The characteristic single-pump parametric amplifier gain spectrum exhibits two main sidebands symmetrically located with respect to the pump frequency. In the phase-insensitive (PI) mode, signal waves to be amplified are injected in the amplifier at frequencies different (blue or red detuned) from the pump one. Idler waves are then spontaneously generated on the other side of the pump frequency due to the nature of the four-wave mixing process. In the phase-sensitive (PS) operational regime [7,8], instead, idlers, with an appropriate phase relation with respect to pump and signals, have to be injected at the amplifier input to provide adequate interference with the signals in order to achieve larger gain. In both scenarios, in the context of optical communications, idlers have to be filtered out after the amplification to prevent detrimental nonlinear interaction during information transmission. Idler amplification is dictated by the signature symmetric nature of the parametric gain spectrum which is governed at the leading order by the second-order dispersion coefficient. Asymmetric gain spectrum in parametric amplifiers has been studied and observed as a consequence of either third-order dispersion [9–11], gain saturation [12], Raman gain [13,14] or asymmetric losses for signal and idler waves [15–17]. However, these asymmetries are not pronounced enough to reduce to a negligible value the idlers gain over a large bandwidth. Multimode fibers offer an appealing alternative way to provide amplification to signals while confining idlers in a separate optical mode. This occurs through the so-called intermodal four-wave mixing process [18–22]. In this work, we demonstrate analytically and numerically a parametric amplifier consisting of a dual-core silica fiber, showing that an operational regime exists where signals carried by one supermode of the system experience substantial gain, while idler waves amplification is negligible

#480480 https://doi.org/10.1364/OE.480480
Journal © 2023 Received 11 Nov 2022; revised 26 Jan 2023; accepted 6 Feb 2023; published 2 Mar 2023

Optics EXPRESS

in the same supermode. The physical principle underpinning this process is the analogue of intermodal four-wave mixing for a multicore fiber system.

Parametric amplification in coupled nonlinear waveguides, suggested in pioneering contributions several decades ago [23,24], can provide broadband flat gain and low noise figure in both PS and PI operational mode [25–27]. It also enables compensation of pump attenuation induced phase-matching degradation via spatially dependent coupling [28]; as well as dispersion compensation through coupling dispersion engineering [29].

In this article, we show instead that coupled-core fibers parametric amplifiers operated in the regime when the two cores are pumped with different power, thanks to the frequency dependency of the coupling, can provide frequency asymmetric gain for the two supermodes of the system. This results in negligible idlers amplification in the supermode carrying the signals, relying on a purely conservative nonlinear dynamics. In Fig. 1 the amplifier concept is illustrated pictorially. Intermodal dispersion has been observed experimentally [30] and also studied in the context of soliton formation and parametric amplification [31,32] in arrays of coupled waveguides. Furthermore, modulation instability in coupled nonlinear Schrödinger equations (NLSEs) has been studied analytically [24,33] including the role of frequency-dependent coupling and in particular of the first order term in its Taylor expansion around the pump frequency [34,35] (see also [36–39] for various generalized cases). However, the remarkable frequency asymmetric gain spectrum for different supermodes which we report here has never been described so far to the best of our knowledge.

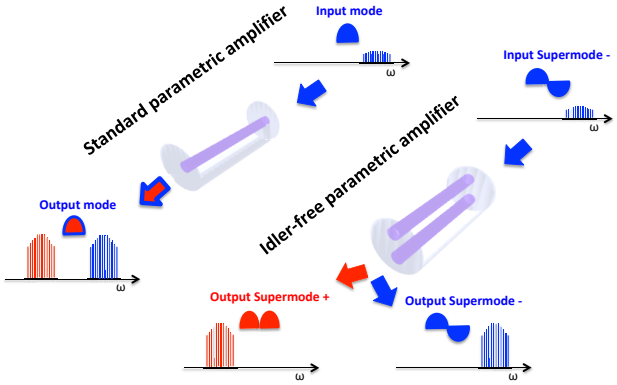

Fig. 1. Amplifier concept. Schematic of the difference between the standard parametric amplifier, which amplifies signals and generates idlers in the same optical mode, and the asymmetrically pumped dual-core fiber parametric amplifier, for which the signals encoded into one supermode are amplified and no idlers are generated in the same supermode.

The model for our system consists of two coupled NLSEs ruling the propagation of the electric field amplitudes $A_{1,2}$ along two identical linearly coupled waveguides:

$$\frac{\partial A_1}{\partial z} = i\sum_{n=0}^{2}\frac{\beta_n}{n!}(i\partial_t)^n A_1 + i\gamma|A_1|^2A_1 + i\sum_{n=0}^{2}\frac{C_n}{n!}(i\partial_t)^n A_2, \tag{1a}$$

$$\frac{\partial A_2}{\partial z} = i\sum_{n=0}^{2}\frac{\beta_n}{n!}(i\partial_t)^n A_2 + i\gamma|A_2|^2A_2 + i\sum_{n=0}^{2}\frac{C_n}{n!}(i\partial_t)^n A_1. \tag{1b}$$

β_n and C_n are the n-th coefficient of the Taylor expansion of the frequency-dependent propagation constant $\beta(\omega)$ and coupling $C(\omega)$ respectively, while γ is the nonlinearity coefficient, t is the temporal coordinate, and z is the spatial evolution coordinate along the longitudinal dimension

Optics EXPRESS

of the waveguides. Despite here we consider only up to second-order Taylor expansions of waveguide and coupling dispersion, our theoretical framework can be naturally generalized to include higher-order terms too. In this system, the four-wave mixing process can be described using 6 coupled equations for the pump ($u_{p1,p2}$), signal ($u_{s1,s2}$) and idler ($u_{i1,i2}$) wave amplitudes oscillating with angular frequency ω_0, $\omega_s = \omega_0 + \Omega$ and $\omega_i = \omega_0 - \Omega$ respectively. In this article, we follow the convention of considering the signals having larger frequency than the pump, i.e. $\Omega>0$ (in Supplement 1, S6, the case of signals red detuned with respect to the pump is discussed too). The equations for waveguide 1 read:

$$\frac{\partial u_{p1}}{\partial z} = \left(i\beta_0 + i\gamma|u_{p1}|^2\right) u_{p1} + iC_0 u_{p2}, \tag{2a}$$

$$\frac{\partial u_{s1}}{\partial z} = \left[i\beta(\omega_s) + 2i\gamma|u_{p1}|^2\right] u_{s1} + iC(\omega_s)u_{s2} + i\gamma u_{p1}^2 u_{i1}^*, \tag{2b}$$

$$\frac{\partial u_{i1}}{\partial z} = \left[i\beta(\omega_i) + 2i\gamma|u_{p1}|^2\right] u_{i1} + iC(\omega_i)u_{i2} + i\gamma u_{p1}^2 u_{s1}^*, \tag{2c}$$

where the small sidebands approximation $|u_{s,i}|^2/|u_p|^2 \ll 1$ has been considered. C_0 is the coupling at the pump frequency. Exchanging the indexes 1 and 2 provides the equations for the second waveguide. We consider the power asymmetric pump waves solution with common initial phase ϕ_0, i.e.

$$u_{p1,p2} = \sqrt{P_{1,2}}e^{i\phi_p}, \quad \phi_p = \phi_0 + \beta_0 z + \gamma P_p z, \tag{3}$$

where $P_{1,2} = \frac{1}{2}(P_p \pm P_d)$, P_p is the total pump power, and $P_d = \sqrt{P_p^2 - (2C_0/\gamma)^2}$ is the power asymmetry parameter. It is important to notice that, unlike the symmetric power stationary solution, the asymmetric one does not exist for arbitrary input power. It requires conditions which are more restrictive — but not prohibitive from an experimental point of view — namely that the total input power should exceed a certain threshold, satisfying $P_p>2C_0/\gamma$. Then, by introducing $e_{s1,s2,i1,i2}(z)$ defined by

$$u_{s1,s2} = e_{s1,s2}e^{i\beta_{\text{odd}}z}e^{i\phi_p}, \quad u_{i1,i2} = e_{i1,i2}e^{-i\beta_{\text{odd}}z}e^{i\phi_p}, \tag{4}$$

where $\beta_{\text{odd}} = [\beta(\omega_s) - \beta(\omega_i)]/2$, (2b) and (2c) can be rewritten as

$$\partial_z \begin{pmatrix} E_+ \\ E_- \end{pmatrix} = iM \begin{pmatrix} E_+ \\ E_- \end{pmatrix} = i \begin{pmatrix} M_+ & M_c \\ M_c & M_- \end{pmatrix} \begin{pmatrix} E_+ \\ E_- \end{pmatrix}. \tag{5}$$

Here we defined $E_\pm = (e_{s\pm}, e_{i\pm}^*)^T = (e_{s1} \pm e_{s2}, e_{i1}^* \pm e_{i2}^*)^T$, so that the sidebands of supermodes $A_\pm = (A_1 \pm A_2)/\sqrt{2}$ can be expressed as

$$A_\pm = \begin{cases} e_{s\pm}e^{i\beta_{\text{odd}}z}e^{i\phi_p}e^{i\Omega t}/\sqrt{2}, & \text{Signal} \\ e_{i\pm}e^{-i\beta_{\text{odd}}z}e^{i\phi_p}e^{-i\Omega t}/\sqrt{2}, & \text{Idler.} \end{cases} \tag{6}$$

The submatrices $M_\pm$, which describe the evolution of $E_\pm$, and M_c, representing the coupling between the modes $E_\pm$ induced by pump power difference P_d, read respectively

$$M_\pm = \begin{pmatrix} K_\pm \pm C_{\text{odd}} & \gamma\frac{P_p}{2} \\ -\gamma\frac{P_p}{2} & -K_\pm \pm C_{\text{odd}} \end{pmatrix}, \quad M_c = \gamma\frac{P_d}{2}\begin{pmatrix} 2 & 1 \\ -1 & -2 \end{pmatrix}, \tag{7}$$

where $K_\pm = \Delta\beta/2 \pm \Delta C/2 \pm C_0$, $\Delta\beta(\Omega) = \beta(\omega_s) + \beta(\omega_i) - 2\beta_0$, $\Delta C(\Omega) = C(\omega_s) + C(\omega_i) - 2C_0$ and $C_{\text{odd}} = [C(\omega_s) - C(\omega_i)]/2$. $E_\pm$ can be computed at an arbitrary propagation distance z as $(E_+(z), E_-(z))^T = N(E_+(0), E_-(0))^T$ with matrix $N = e^{iMz}$.

Optics EXPRESS

We now focus on the input regime where signal waves have opposite phases in two coupled waveguides so that $e_{s1}(0) + e_{s2}(0) = 0$ and study the output of the supermode A_-. Thus the gain spectrum for the sidebands can be defined as

$$G(z) = \begin{cases} |e_{s-}(z)|^2/|e_{s-}(0)|^2, & \text{Signal} \\ |e_{i-}(z)|^2/|e_{s-}(0)|^2, & \text{Idler.} \end{cases} \tag{8}$$

According to our definition of the gain, $G(z)<1$, at the amplifier output for idlers implies that idlers have not reached a power equal to the input signals. Firstly we considered $C_2 = 0$ to better highlight the necessary conditions for idler-free parametric amplification. We have compared the analytical predictions with numerical simulations of the coupled NLSEs (Eqs. (1)) performed using a split-step Fourier algorithm. In the PI regime, considering $e_{i1}(0) = e_{i2}(0) = 0$, the analytical gain reads

$$G_{\mathrm{PI}}(z) = \begin{cases} |N_{33}(z)|^2, & \text{Signal} \\ |N_{43}(z)|^2, & \text{Idler} \end{cases} \tag{9}$$

where N_{ij} is the element of the matrix N at i-th row and j-th column. The matrix elements need to be calculated numerically due to their cumbersome form resulting from the matrix exponential e^{iMz}.

We show the dependence of the amplifier gain spectrum versus C_1 in Fig. 2 for anomalous (a) and normal (b) waveguide dispersion respectively, while an example of the idler-free operation for the A_- supermode is shown in panels c) and d). In the latter case, the idler-free operational mode is limited to the high-frequency range only, and the signal gain is smaller for the parameters considered. For the particular parameters selected, the idler-free regime exhibits a remarkable ≈20 dB gain difference between signal and idler sidebands in the anomalous and in the normal dispersion regime too. As in the normal dispersion scenario, the asymmetric gain coexists with symmetric low-frequency sidebands — which would require additional filtering — to quantify the amount of useful signal power contained in the idler-free spectral lobe, for input signal waves in the interval $(0, \Omega_m]$, we have computed the following quantities: $I_+ = \int_0^{+\Omega_m} S_-(\Omega')d\Omega' \Big/ \int_{-\Omega_m}^{+\Omega_m} S_-(\Omega')d\Omega'$ and $I_s = \int_{s1}^{s2} S_-(\Omega')d\Omega' \Big/ \int_{-\Omega_m}^{+\Omega_m} S_-(\Omega')d\Omega'$. I_+ is the ratio between the integral of the output spectral power $S_-(\Omega')$ of the supermode A_- computed for frequencies larger than the pump one and the total power contained in the full simulations window $[-\Omega_m = -2\pi \cdot 6, +\Omega_m = 2\pi \cdot 6]$ rad/ps, excluding the pump. I_s is the ratio between the integral of the supermode A_- output spectral power computed in the interval around the asymmetric signal spectral lobe delimited by s_1 and s_2 and the total power contained in the full simulations window. For the anomalous dispersion case — (Fig. 2(c)) with $C_1 = -7.5$ ps $\cdot$ km^{-1} — we obtain $I_+ = 0.96$ and $I_s = 0.79$ meaning that 96% of the power of A_- supermode is contained in the signal spectrum and that 79% of the power is in the asymmetric spectral lobe in the interval $[s_1 = 2\pi \cdot 3.85, s_2 = 2\pi \cdot 5.61]$ rad/ps. Performances are less significant in the normal dispersion regime — (Fig. 2(d)) with $C_1 = 7.5$ ps $\cdot$ km^{-1} — due to large power contained in the low-frequency symmetric sidebands. In that case, we obtain $I_+ = 0.58$ and $I_s = 0.9$ meaning that 58% of the power of A_- supermode is contained in the signal spectrum and that 9% of the power is in the asymmetric spectral lobe in the interval $[s_1 = 2\pi \cdot 4.10, s_2 = 2\pi \cdot 5.53]$ rad/ps. Similar results are obtained for the PS amplifier shown below.

The PS operational mode in two coupled waveguides parametric amplifiers can be implemented in various different scenarios [25,26]. Here, without loss of generality, we focus on the initial condition: $e_{s1}(0) = e_{i1}(0) = -e_{s2}(0) = -e_{i2}(0)$, and assume that the initial phase of signal wave in waveguide 1 is $\phi_s + \phi_0$, then the gain reads:

Optics EXPRESS

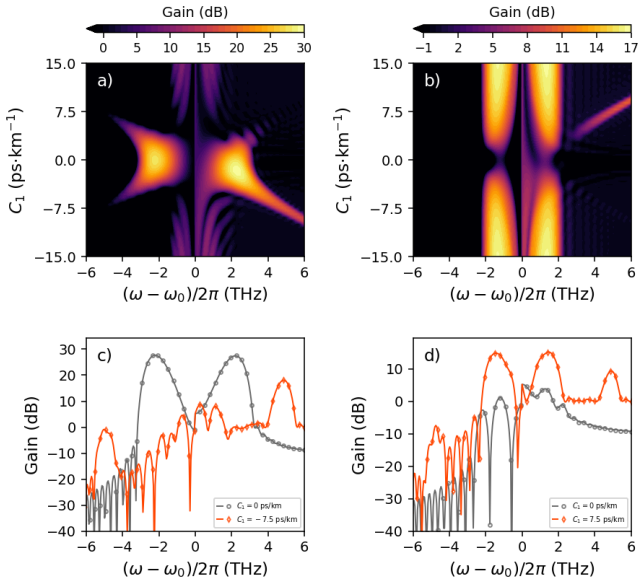

Fig. 2. PI amplifier. Map of analytical parametric gain for A_- versus frequency and C_1 in anomalous a) and normal b) dispersion regime, and comparison of gain spectrum versus frequency between theory (continuous line) and numerics (dots) for anomalous c) and normal d) dispersion regime with $C_1 = \mp 7.5$ ps $\cdot$ km^{-1} ($C_1 = 0$) shown in orange (gray). Other parameters used are $\beta_2 = \mp 0.5$ ps^{2}km^{-1}, $\gamma = 10$ W^{-1}km^{-1}, $P_p = 5.4$ W, $C_0 = 15$ km^{-1}, $C_2 = 0$, and $z = 0.1$ km.

$$G_{\mathrm{PS}}(z) = \begin{cases} |N_{33}(z)e^{i\phi_s} + N_{34}(z)e^{-i\phi_s}|^2, & \text{Signal} \\ |N_{43}(z)e^{i\phi_s} + N_{44}(z)e^{-i\phi_s}|^2, & \text{Idler.} \end{cases} \tag{10}$$

The characterization of the PS amplifier is shown in Fig. 3. We have furthermore investigated the dependency of the gain spectrum on the pump power difference P_d which is shown in Fig. 4 for both PI and PS operational mode, as playing with pump power is a practical way to control the amplifier gain experimentally. Results show that there is a trade-off between maximizing the gain and keeping negligible idler amplification. It is important to stress that the gain asymmetry for signal and idler waves between different supermodes reported in this work is not related to odd dispersion terms β_{odd}, which in our system results in a simple phase factor as it can be appreciated from Eq. (4). Furthermore, while the impact of C_1 on the MI spectrum in asymmetrically pumped dual-core fibers has been investigated in [34,35], in those works the frequency asymmetric gain spectrum for different supermodes was not observed, possibly because the focus was on the eigenvalue spectrum of the continuous wave stability problem (which is symmetric in frequency) and the parametric gain was not calculated by fully solving the signals and idlers equations. Both in the PI and PS regime, the amplifier asymmetric gain spectrum is due to the combined action of the unbalanced pump power distribution between the two waveguides and of the frequency dependency of the coupling. Notably, $P_d \neq 0$ causes supermodes mixing as it can be clearly seen from Eqs. (5) and (7) showing that the supermode coupling matrix M_c is nonvanishing only if $P_d \neq 0$. In that case, even if one supermode only is injected inside the amplifier, the nonlinear dynamics couples energy into the other supermode too. If $C_1 \neq 0$ too, while the four-wave mixing process keeps its symmetric spectral feature, then the signals remain located in one supermode while the idlers are located in the other supermode. In S2 of Supplement 1 we prove this point by showing indeed examples of the gain spectrum for the sidebands of supermode A_+ obtained for the same parameters of Fig. 2, which corresponds to initial conditions

Optics EXPRESS

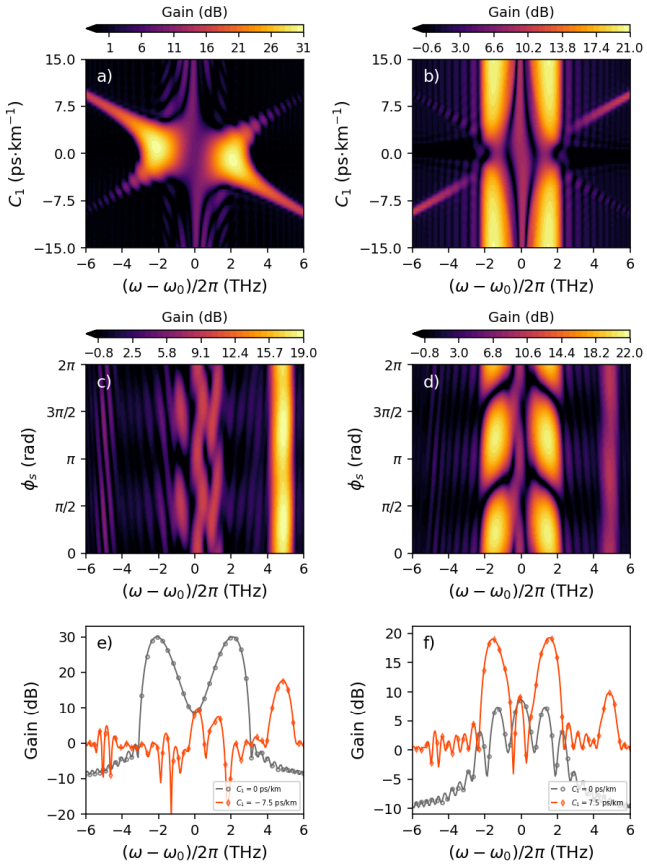

Fig. 3. PS amplifier. Map of analytical parametric gain for A_- versus frequency and C_1 in anomalous a) and normal b) dispersion regime with $\phi_s = 0$, and versus frequency and ϕ_s in anomalous c) and normal d) dispersion regime with $C_1 = \mp 7.5$ ps $\cdot$ km^{-1}; gain spectrum versus frequency comparison between theory (continuous line) and numerics (dots) for anomalous e) and normal f) dispersion regime with $\phi_s = 0$ and $C_1 = \mp 7.5$ps $\cdot$ km^{-1} ($C_1 = 0$) shown in orange (gray). Remaining parameters are like in Fig. 2.

($e_{s+}(0) = 0$, $e_{s-}(0) \neq 0$), and similarly the gain for A_- and A_+ with initial conditions ($e_{s+}(0) \neq 0$, $e_{s-}(0) = 0$) too. We stress again that for normal dispersion the signal-idler separation between supermodes is not complete and it does not apply in the low-frequency range. This makes the anomalous dispersion regime the most attractive for a full separation of signals and idlers. An analytical expression for the gain difference in dB between the two supermodes as a function of the dominant eigenvector $\mathbf{v}_1 = (v_1, v_2, v_3, v_4)^T$ of matrix M has been derived (see Supplement 1, S7) and reads: $G_{\pm}^{\text{diff}} = 10 \log \frac{|e_{s\pm}|^2}{|e_{i\pm}|^2} = 10 \log \left| \frac{v_{2\mp 1}}{v_{3\mp 1}} \right|^2$. A further intuitive picture of the reason for the frequency asymmetric gain of the two supermodes can be provided by considering that in the asymmetric operational regime signal waves for the individual waveguides modes ($u_{s1,s2}$) exhibit a π phase difference, while idlers ($u_{i1,i2}$) have no phase difference (see Supplement 1, S8). We can attribute the origin of this phase-shift to the interplay between the asymmetric pump power distribution between the two cores and C_{odd} — the odd part of the frequency dependent coupling — which are the necessary ingredients for the intermodal four-wave mixing to occur. As supermodes "±" are defined by the sum/difference between individual waveguides modes respectively, i.e., $A_\pm = (A_1 \pm A_2)/\sqrt{2}$, this unequal phase difference translates, due to

Optics EXPRESS

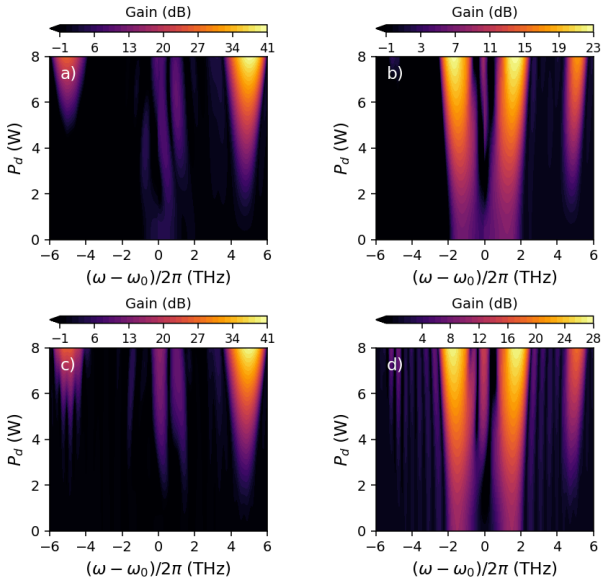

Fig. 4. P_d-dependency. Map of PI analytical parametric gain for A_- versus frequency and P_d in anomalous a) and normal b) dispersion regime; and map of PS parametric analytical gain versus frequency and P_d in anomalous c) and normal d) dispersion regime with $\phi_s = 0$. Other parameters used are $C_1 = \mp 7.5$ ps $\cdot$ km^{-1}, $\beta_2 = \mp 0.5$ ps^{2}km^{-1}, $\gamma = 10$ W^{-1}km^{-1}, $C_0 = 15$ km^{-1}, $C_2 = 0$, and $z = 0.1$ km. The variation of P_d depicted corresponds to a change of P_p in the interval $[3, 8.5]$ W.

interference, into the fact that one supermode is idler-free and the other one is signal-free (at least in a certain frequency bandwidth). While the supermode carrying the signals can be used for idler-free amplification purpose, the supermode carrying the idlers, A_+ in our examples, can be used for wavelength conversion applications. The two supermodes can be easily extracted at the amplifier output by a simple combination of a phase shifter and a coupler, as shown in S1 of Suppelment 1, where a potential experimental setup schematic is illustrated. Presence of coupling second-order dispersion ($C_2 \neq 0$) and changing magnitude of waveguide dispersion (β_2) do not affect qualitatively and significantly the amplifier performances and their impact is briefly summarised in Supplement 1, S4 and S5.

We have furthermore verified through numerical simulations that the undepleted pump approximation assumed in the analytical theory is excellent for the parameters used in this study (input signals power $\sim 10^{-12}$ W) as pump depletion is negligible, resulting in an about 10^{-9}% of pump power reduction between output and input. The validity of this assumption can also be appreciated indirectly from the nice agreement between theory and simulations across the whole paper.

In conclusion, we have described parametric amplification enabled by intermodal four-wave mixing in a dual-core optical fiber. We have shown how the interplay between frequency-dependent coupling and pump power unbalance in two coupled nonlinear waveguides constitutes the leading factor to achieve signals and idler separation through a frequency asymmetric gain for the two system supermodes. We have shown that the latter is possible for realistic dual-core fiber parameters. Our rigorous analytical theory, in excellent agreement with numerical simulation results, will provide a guide for future design of experimental demonstrations of the concept presented, for optimising idler-free amplifier performances (including bandwidth, maximum gain, energy efficiency), and for studying possible impairments. Furthermore, our framework

Optics EXPRESS

can be adapted to describe coupled waveguides made of different materials such as silicon and silicon nitride. The results discussed in this work will potentially enable a more efficient use of the bandwidth in optical parametric amplification and may find applications for wavelength conversion too.

Funding. Engineering and Physical Sciences Research Council (EP/W002868/1); Royal Academy of Engineering (Research Fellowship Scheme).

Disclosures. The authors declare no conflicts of interest.

Data availability. Data underlying the results presented in this paper are not publicly available at this time but may be obtained from the authors upon reasonable request.

Supplemental document. See Supplement 1 for supporting content.

References

1. M. E. Mahric, *Fiber Optical Parametric Amplifiers, Oscillators and Related Devices: Theory, Applications, and Related Devices* (Cambridge University Press, 2007).
2. J. Hansryd, P. A. Andrekson, M. Westlund, J. Li, and P. O. Hedekvist, "Fiber-based optical parametric amplifiers and their applications," IEEE J. Sel. Top. Quantum Electron. **8**(3), 506–520 (2002).
3. R. Stolen and J. Bjorkholm, "Parametric amplification and frequency conversion in optical fibers," IEEE J. Quantum Electron. **18**(7), 1062–1072 (1982).
4. Z. Ye, P. Zhao, K. Twayana, M. Karlsson, V. Torres-Company, and P. A. Andrekson, "Overcoming the quantum limit of optical amplification in monolithic waveguides," Sci. Adv. **7**(38), eabi8150 (2021).
5. P. Zhao, M. Karlsson, and P. A. Andrekson, "Low-noise integrated phase-sensitive waveguide parametric amplifiers," J. Lightwave Technol. **40**(1), 128–135 (2022).
6. P. Zhao, Z. Ye, M. Karlsson, V. Torres-Company, and P. A. Andrekson, "Low-noise phase-sensitive parametric amplifiers based on integrated silicon-nitride-waveguides for optical signal processing," J. Lightwave Technol. **40**(6), 1847–1854 (2022).
7. P. A. Andrekson and M. Karlsson, "Fiber-based phase-sensitive optical amplifiers and their applications," Adv. Opt. Photonics **12**(2), 367–428 (2020).
8. S. Olsson, H. Eliasson, E. Astra, M. Karlsson, and P. A. Andrekson, "Long-haul optical transmission link using low-noise phase-sensitive amplifiers," Nat. Commun. **9**(1), 2513 (2018).
9. A. Mussot, E. Louvergneaux, N. Akhmediev, F. Reynaud, L. Delage, and M. Taki, "Optical fiber systems are convectively unstable," Phys. Rev. Lett. **101**(11), 113904 (2008).
10. M. I. Kolobov, A. Mussot, A. Kudlinski, E. Louvergneaux, and M. Taki, "Third-order dispersion drastically changes parametric gain in optical fiber systems," Phys. Rev. A **83**(3), 035801 (2011).
11. M. Droques, B. Barviau, A. Kudlinski, M. Taki, A. Boucon, T. Sylvestre, and A. Mussot, "Symmetry-breaking dynamics of the modulational instability spectrum," Opt. Lett. **36**(8), 1359–1361 (2011).
12. Z. Lali-Dastjerdi, K. Rottwitt, M. Galili, and C. Peucheret, "Asymmetric gain-saturated spectrum in fiber optical parametric amplifiers," Opt. Express **20**(14), 15530–15539 (2012).
13. A. S. Y. Hsieh, G. K. L. Wong, S. G. Murdoch, S. Coen, F. Vanholsbeeck, R. Leonhardt, and J. D. Harvey, "Combined effect of raman and parametric gain on single-pump parametric amplifiers," Opt. Express **15**(13), 8104–8114 (2007).
14. V. Gordienko, M. F. C. Stephens, A. E. El-Taher, and N. J. Doran, "Ultra-flat wideband single-pump raman-enhanced parametric amplification," Opt. Express **25**(5), 4810–4818 (2017).
15. T. Tanemura, Y. Ozeki, and K. Kikuchi, "Modulational instability and parametric amplification induced by loss dispersion in optical fibers," Phys. Rev. Lett. **93**(16), 163902 (2004).
16. A. M. Perego, S. K. Turitsyn, and K. Staliunas, "Gain through losses in nonlinear optics," Light: Sci. Appl. **7**(1), 43 (2018).
17. R. El-Ganainy, J. I. Dadap, and R. M. Osgood, "Optical parametric amplification via non-hermitian phase matching," Opt. Lett. **40**(21), 5086–5089 (2015).
18. R. Stolen, "Phase-matched-stimulated four-photon mixing in silica-fiber waveguides," IEEE J. Quantum Electron. **11**(3), 100–103 (1975).
19. R.-J. Essiambre, M. A. Mestre, R. Ryf, A. H. Gnauck, R. W. Tkach, A. R. Chraplyvy, Y. Sun, X. Jiang, and R. Lingle, "Experimental investigation of inter-modal four-wave mixing in few-mode fibers," IEEE Photonics Technol. Lett. **25**(6), 539–542 (2013).
20. H. Pourbeyram, E. Nazemosadat, and A. Mafi, "Detailed investigation of intermodal four-wave mixing in smf-28: blue-red generation from green," Opt. Express **23**(11), 14487–14500 (2015).
21. Y. Xiao, R.-J. Essiambre, M. Desgroseilliers, A. M. Tulino, R. Ryf, S. Mumtaz, and G. P. Agrawal, "Theory of intermodal four-wave mixing with random linear mode coupling in few-mode fibers," Opt. Express **22**(26), 32039–32059 (2014).
22. S. M. M. Friis, I. Begleris, Y. Jung, K. Rottwitt, P. Petropoulos, D. J. Richardson, P. Horak, and F. Parmigiani, "Inter-modal four-wave mixing study in a two-mode fiber," Opt. Express **24**(26), 30338–30349 (2016).

Optics EXPRESS

23. A. Mecozzi, "Parametric amplification and squeezed-light generation in a nonlinear directional coupler," Opt. Lett. **13**(10), 925–927 (1988).
24. S. Trillo, S. Wabnitz, G. I. Stegeman, and E. M. Wright, "Parametric amplification and modulational instabilities in dispersive nonlinear directional couplers with relaxing nonlinearity," J. Opt. Soc. Am. B **6**(5), 889–900 (1989).
25. V. Ribeiro, M. Karlsson, and P. Andrekson, "Parametric amplification with a dual-core fiber," Opt. Express **25**(6), 6234–6243 (2017).
26. V. Ribeiro, A. Lorences-Riesgo, P. Andrekson, and M. Karlsson, "Noise in phase-(in)sensitive dual-core fiber parametric amplification," Opt. Express **26**(4), 4050–4059 (2018).
27. V. Ribeiro, A. D. Szabó, A. M. Rocha, C. B. Gaur, A. A. I. Ali, Y. Quiquempois, A. Mussot, G. Bouwmans, and N. Doran, "Parametric amplification and wavelength conversion in dual-core highly nonlinear fibers," J. Lightwave Technol. **40**(17), 6013–6020 (2022).
28. V. Ribeiro and A. M. Perego, "Parametric amplification in lossy nonlinear waveguides with spatially dependent coupling," Opt. Express **30**(10), 17614–17624 (2022).
29. M. Shi, V. Ribeiro, and A. M. Perego, "Parametric amplification in coupled nonlinear waveguides: the role of coupling dispersion," *submitted for publication* (2022).
30. K. Chiang, Y. Chow, D. Richardson, D. Taverner, L. Dong, L. Reekie, and K. Lo, "Experimental demonstration of intermodal dispersion in a two-core optical fibre," Opt. Commun. **143**(4-6), 189–192 (1997).
31. C. J. Benton and D. V. Skryabin, "Coupling induced anomalous group velocity dispersion in nonlinear arrays of silicon photonic wires," Opt. Express **17**(7), 5879–5884 (2009).
32. C. E. de Nobriga, G. D. Hobbs, W. J. Wadsworth, J. C. Knight, D. V. Skryabin, A. Samarelli, M. Sorel, and R. M. D. L. Rue, "Supermode dispersion and waveguide-to-slot mode transition in arrays of silicon-on-insulator waveguides," Opt. Lett. **35**(23), 3925–3927 (2010).
33. R. S. Tasgal and B. A. Malomed, "Modulational instabilities in the dual-core nonlinear optical fiber," Phys. Scr. **60**(5), 418–422 (1999).
34. J. H. Li, K. S. Chiang, and K. W. Chow, "Modulation instabilities in two-core optical fibers," J. Opt. Soc. Am. B **28**(7), 1693–1701 (2011).
35. J. H. Li, K. S. Chiang, B. A. Malomed, and K. W. Chow, "Modulation instabilities in birefringent two-core optical fibres," J. Phys. B: At., Mol. Opt. Phys. **45**(16), 165404 (2012).
36. K. Nithyanandan, R. V. J. Raja, and K. Porsezian, "Modulational instability in a twin-core fiber with the effect of saturable nonlinear response and coupling coefficient dispersion," Phys. Rev. A **87**(4), 043805 (2013).
37. A. A. Nair, K. Porsezian, and M. Jayaraju, "Impact of higher order dispersion and nonlinearities on modulational instability in a dual-core optical fiber," Eur. Phys. J. D **72**(1), 6 (2018).
38. J. H. Li, T. T. Sun, Y. Q. Ma, Y. Chen, Z. L. Cao, F. L. Xian, D. Z. Wang, and W. Wang, "Modulation instabilities in nonlinear two-core optical fibers with fourth order dispersion," Optik **208**, 164134 (2020).
39. J. H. Li, T. T. Sun, Y. Q. Ma, Y. Y. Chen, Z. L. Cao, and F. L. Xian, "The effects of fourth-order dispersion on modulation instabilities in two-core optical fibers with asymmetric CW state," Phys. Scr. **95**(11), 115502 (2020).